



Published in final edited form as:

*Bone*. 2017 October ; 103: 1–11. doi:10.1016/j.bone.2017.06.004.

## Splenomegaly, myeloid lineage expansion and increased osteoclastogenesis in osteogenesis imperfecta murine

Brya G Matthews<sup>1,\*</sup>, Emilie Roeder<sup>1</sup>, Xi Wang<sup>1</sup>, Hector Leonardo Aguila<sup>2</sup>, S. Kyeong Lee<sup>3</sup>, Danka Grcevic<sup>4</sup>, and Ivo Kalajzic<sup>1,\*</sup>

<sup>1</sup>Department of Reconstructive Sciences, University of Connecticut, Farmington, CT 06030, USA

<sup>2</sup>Department of Immunology, University of Connecticut, Farmington, CT 06030, USA

<sup>3</sup>Center on Aging, University of Connecticut, Farmington, CT 06030, USA

<sup>4</sup>Department of Physiology and Immunology, School of Medicine, University of Zagreb, Zagreb 10000, Croatia

### Abstract

Osteogenesis imperfecta (OI) is a disease caused by defects in type I collagen production that results in brittle bones. While the pathology is mainly caused by defects in the osteoblast lineage, there is also elevated bone resorption by osteoclasts resulting in high bone turnover in severe forms of the disease. Osteoclasts originate from hematopoietic myeloid cells, however changes in hematopoiesis have not been previously documented in OI. In this study, we evaluated hematopoietic lineage distribution and osteoclast progenitor cell frequency in bone marrow, spleen and peripheral blood of osteogenesis imperfecta murine (OIM) mice, a model of severe OI. We found splenomegaly in all ages examined, and expansion of myeloid lineage cells (CD11b<sup>+</sup>) in bone marrow and spleen of 7–9 week old male OIM animals. OIM spleens also showed an increased frequency of purified osteoclast progenitors. This phenotype is suggestive of chronic inflammation. Isolated osteoclast precursors from both spleen and bone marrow formed osteoclasts more rapidly than wild-type controls. We found that serum TNF $\alpha$  levels were increased in OIM, as was IL1 $\alpha$  in OIM females. We targeted inflammation therapeutically by treating growing animals with murine TNFR2:Fc, a compound that blocks TNF $\alpha$  activity. Anti-TNF $\alpha$  treatment marginally decreased spleen mass in OIM females, but failed to reduce bone resorption, or improve bone parameters or fracture rate in OIM animals. We have demonstrated that OIM mice have changes in their hematopoietic system, and form osteoclasts more rapidly

**Corresponding authors:** Brya G Matthews, Department of Reconstructive Sciences, MC 3705, School of Dental Medicine, University of Connecticut, 263 Farmington Ave, Farmington, CT 06030. Tel.: 860-679-3462; bmatthews@uchc.edu, Ivo Kalajzic, Department of Reconstructive Sciences, MC 3705, School of Dental Medicine, University of Connecticut, 263 Farmington Ave, Farmington, CT 06030. Tel.: 860-679-6051; ikalaj@uchc.edu.

**Publisher's Disclaimer:** This is a PDF file of an unedited manuscript that has been accepted for publication. As a service to our customers we are providing this early version of the manuscript. The manuscript will undergo copyediting, typesetting, and review of the resulting proof before it is published in its final citable form. Please note that during the production process errors may be discovered which could affect the content, and all legal disclaimers that apply to the journal pertain.

### Disclosures

The authors have nothing to disclose

Authors' roles: Study design: BGM, HLA, SKL, DG, IK; Data collection: BGM, ER, XW, HLA, DG, IK; Data analysis BGM, HLA, DG; Data interpretation: BGM, HLA, SKL, DG, IK; Drafting manuscript: BGM; Revising manuscript content: IK, HLA, DG; Manuscript approval: all authors

even in the absence of OI osteoblast signals, however therapy targeting TNF $\alpha$  did not improve disease parameters.

## Keywords

Osteogenesis imperfecta; osteoclast; tumor necrosis factor alpha; inflammation

---

## 1. Introduction

Osteogenesis imperfecta (OI) is a genetic disease affecting around 1:10,000 births that is characterized by bone fragility and frequent fractures. OI is caused by defects in type I collagen production or assembly. The majority of cases are caused by mutations in one of the type I collagen genes. While there is a wide range of clinical severity, the disease can cause significant disability and require continuing medical and surgical care. The primary defect causing brittle bones is in the osteoblast lineage, but in more severe forms of OI there is also high bone turnover with increased bone resorption [1]. This feature is also seen in a number of mouse models of type III or type IV OI, including OIM, Brl and Aga2 mice [2–4].

Osteoclasts differentiate through the combined actions of macrophage colony stimulating factor (M-CSF) and receptor activator of nuclear factor kappa B ligand (RANKL). However, it is well established that inflammatory cytokines such as TNF $\alpha$  can act synergistically with RANKL to stimulate increased osteoclastogenesis [5]. This is a major mechanism of both local and systemic bone loss in rheumatoid arthritis (RA), as well as a number of other inflammatory conditions. There is evidence that inflammation may be associated with OI. Patients often have increased body temperature, and elevated prostaglandin E2 in serum has been reported [6, 7]. A recent study also found increased TNF $\alpha$  expression in peripheral blood mononuclear cells from children with OI [8]. However, inflammation as a feature of OI pathophysiology, and as a potential therapeutic target has not been explored in animal models.

Osteogenesis imperfecta murine (OIM) is a widely used murine OI model that lacks functional collagen type I alpha 2 chain. The main characteristics of these mice include small body size, spontaneous fractures, and reduced bone density and strength, similar to type III OI [2, 9–11]. Previous studies in OIM mice have shown that OIM osteoblasts stimulate increased osteoclastogenesis through a RANKL-independent mechanism [12]. However, increased osteoclastogenesis can also be observed in osteoblast-free cultures from both OIM and Brl mice, suggesting a potential osteoblast-independent mechanism for increased osteoclastogenesis in OI [4, 13]. These studies did not evaluate the number of osteoclast progenitors (OCPs) in mice with OI, or whether the OCPs are more sensitive to osteoclastogenic stimuli. Methods are now available to identify and purify OCP populations in bone marrow and peripheral tissues [14, 15]. We therefore sought to study whether OIM mice have changes in OCP frequency in both bone marrow and peripheral tissues, and in parallel conducted a careful dissection of other components of the hematopoietic system.

To date, pharmacological treatments for OI have been limited to anti-resorptive drugs, primarily bisphosphonates. Clinical trials have indicated that bisphosphonates improve bone mineral density (BMD), but do not necessarily reduce fracture rates in OI patients [16, 17]. In addition, because bisphosphonates remain bound to the bone for long periods of time, their use can result in potential problems, such as impairment of metaphyseal remodeling during growth, and poor bone repair following osteotomy [18, 19]. In search of alternative treatment options, a recent study explored the use of denosumab (RANKL neutralizing antibody) in a small number of children with OI, and reported increased BMD, indicating that this antiresorptive agent may also show efficacy in OI [20]. However, there is a need for alternative treatment options. The only bone anabolic drug that is currently approved, PTH, is contraindicated in children. Sclerostin neutralizing antibodies have been trialed in a number of mouse studies, and have generally had positive effects making this a promising target for future human studies [21–25]. TGF $\beta$  neutralizing antibodies also caused dramatic improvement in bone density in strength in both a recessive model of OI (Crtap knockout) and in a mouse with a dominant collagen mutation, representing a novel paradigm for OI treatment by targeting dysregulated matrix-mediated signaling [26].

Previous studies in our lab identified increased TNF $\alpha$  expression as a potential mechanism for increased osteoclast formation in OI cultures [12]. Biologicals targeting TNF $\alpha$  have been in clinical use for over 10 years for diseases such as RA, and are approved for use in children with conditions such as juvenile idiopathic arthritis. Treatment with anti-TNF $\alpha$  agents improves BMD in patients with RA, at least in some studies, primarily due to reduction in inflammation [27]. In the current study, we have found a tendency towards elevated serum levels of TNF $\alpha$ , and indications of increased inflammatory features in OIM animals. This led us to evaluate the effect of the anti-TNF $\alpha$  treatment TNFR2:Fc on bone parameters in OIM mice during adolescent growth.

## 2. Methods

### 2.1 Mice

All procedures were approved by the UConn Health Institutional Animal Care and Use Committee and performed in an AAALACi accredited facility. OIM mice were obtained from Jackson Labs (Bar Harbor, ME) in a mixed background (B6C3Fe *a/a-Coll1a2<sup>oim</sup>/J*). Mice were group housed in individually ventilated cages (Thoren Caging, Hazleton, PA) with a photoperiod of 12:12. The room temperature and humidity were maintained at 22°C and 30–70% respectively. Mice were fed irradiated Rodent Diet (Teklad 2918, Invigo, Indianapolis, IN), made available in both pellets and crushed form, and water (reverse-osmosis) ad libitum. Vendor surveillance and colony sentinel monitoring results show that the colony is free from all pathogens tested. The majority of experimental animals were generated by crossing heterozygous animals, although some OI mice were generated by crossing OI  $\times$  OI. Genotypes were determined by PCR as previously described [28]. The presence of fractures in OI mice was determined by imaging with a Faxitron digital X-ray (Faxitron Bioptics, Tucson, AZ, USA).

## 2.2 Tissue collection and processing

Blood for serum was collected under ketamine-xylazine anesthesia via the retro-orbital sinus following at least 6h starvation. Following coagulation for 30 minutes, samples were centrifuged and serum collected and stored. Blood for flow cytometry analysis was collected into 1mM EDTA in PBS, pH 7.4, and red blood cells (RBC) sedimented in 2% dextran. Spleens were isolated, weighed, and single cell suspensions were obtained by crushing the organ between two frosted glass slides and resuspending in staining media (SM, 1×HBSS 10mM HEPES 2% FBS). RBCs were lysed by hypotonic shock using ACK buffer (155mM NH<sub>4</sub>Cl, 10mM KHCO<sub>3</sub>, 0.1mM EDTA) for 5 minutes, then cells were washed and passed through a 70µm cell strainer prior to counting. Bone marrow (BM) was collected from femora and tibiae by flushing with SM followed by RBC lysis and filtration through a 70µm cell strainer. OI bones with severe fractures were not used for bone marrow collection.

## 2.3 Flow cytometry and cell sorting

Isolated cell suspensions were stained for multiple hematopoietic markers, including OCPs, as previously described, using commercially available antibodies [14, 15, 29]. Multiparameter flow cytometry analysis was performed on samples from individual animals. Data were collected on LSRII or FACSAria II instruments (BD Biosciences), and analyzed using FlowJo software. For cell sorting, samples were generally pooled from 2–3 mice prior to staining. Spleen samples were depleted of lymphoid cells using anti-APC magnetic beads (Miltenyi Biotech, Bergisch Gladbach, Germany). Sorting was performed on a FACSAria II using an 85µm nozzle.

## 2.4 Osteoclast culture

Cells were seeded in 96-well plates in αMEM 10% FBS + 30ng/ml M-CSF + 30ng/ml RANKL (R&D Systems, Minneapolis, MN). Sorted bone marrow OCPs were seeded at a density of 1000 cells/well, sorted spleen OCPs at 10,000 cells/well and total spleen cells at 100,000 cells/well. Media were changed every 3 days. At the completion of culture (day 3–5 for bone marrow, day 5–7 for spleen due to slower differentiation of spleen cells [14, 15]), cultures were fixed for 15 minutes in 2.5% glutaraldehyde, and TRAP staining was performed using the Leukocyte Acid Phosphatase Kit (Sigma Aldrich). Osteoclasts were defined as TRAP+ cells with 3 or more nuclei, and were counted manually in each well. Each experimental group contained 5–8 wells.

## 2.5 TNFα neutralizing treatment

Murine TNFR2:Fc was administered to mice to neutralize TNFα (Amgen, Thousand Oaks, CA). OIM mice were randomly assigned to receive either TNFR2:Fc or vehicle (saline) treatment. Body weight and BMD at baseline were not significantly different between groups. Treatment was initiated at 4–5 weeks of age, for a total of 6 weeks. TNFR2:Fc was administered twice a week at a dose of 5µg/g body weight. A small number of wild-type (WT) mice received TNFR2:Fc, and all experiments included vehicle-treated WT mice as controls. X-rays and dual beam X-ray absorptiometry (DXA) scans were performed prior to starting treatment. Bodyweights were measured weekly, and drug dosage adjusted accordingly. Mice were sacrificed a week after the final treatment, X-rays and DXA

measurements were repeated, and tissues collected. Three cohorts of mice underwent treatment at different times. One mouse died during the treatment protocol (male OIM vehicle group), and one was excluded due to failure to gain weight over a 3-week period (female OIM anti-TNF group). Fracture counts were performed using digital X-rays by two independent observers who were blinded to the treatment group. Fractures in the limbs and pelvis were counted. Fractures that had healed such that cortical bone was continuous and no callus was apparent, even if some residual deformity was evident, were not counted.

## 2.6 DXA and micro computed tomography

DXA was performed using a Piximus Mouse 11 densitometer (GE Medical Systems, Madison, WI). Mice were anaesthetized using ketamine-xylazine prior to scanning. Whole body minus head analysis was performed using the software provided. Micro CT was performed on femurs by the UConn Health Micro CT imaging facility with a  $\mu$ CT40 instrument (Scanco). The technician performing scans and analysis was blinded to the treatment group, but not genotype of the mice. A number of bones from OIM mice were excluded from analysis due to the presence of fractures, or other abnormalities that made standard analysis difficult. Bones were scanned with a 16 $\mu$ m voxel size, and standard trabecular and cortical morphometry analysis was performed.

## 2.7 ELISA

ELISA was performed on serum samples. CTX was measured using the RatLaps CTX-I EIA kit (Immunodiagnostic Systems, Tyne & Wear, UK), OIM serum was diluted up to 1:8 to ensure values fell within the standard curve. Cytokines were measured with Mouse TNF $\alpha$  Quantikine High Sensitivity ELISA kit and Mouse IL1 $\alpha$  Quantikine ELISA kit (R&D Systems). All assays were performed according to the manufacturer's instructions.

## 2.8 Statistical analysis

Males and females were analyzed separately in all studies. Exact n values for all groups are shown in Supplemental table 1. OIM data was compared to the appropriate WT control data using Student's t-test. TNF $\alpha$  neutralizing studies were designed to have 90% power to detect a 30% decrease in CTX based on variation found in preliminary studies which indicated n=8/group were required. However, we used more animals in some groups when available to allow for exclusion of bones with fractures from micro CT analysis. Data were analyzed by 1-way ANOVA.

# 3. Results

## 3.1 Changes to hematopoietic composition in OIM mice

In order to examine the hematopoietic compartment in OIM mice, we evaluated cohorts of animals between 5 and 20 weeks of age. We confirmed that OIM animals in our colony had reduced bodyweight in comparison to WT controls (Figure 1A), consistent with previous reports [10]. Macroscopic evaluation of the spleens indicated that OIM mice show splenomegaly in both sexes beginning around sexual maturity and persisting until at least 20 weeks of age (Figure 1B–C). In males aged 7–9 weeks, the spleen weights were significantly increased even without correction for bodyweight (Figure 1C). The cell counts obtained

from the spleens correlated closely with the spleen weight (data not shown, Supplemental table 2), indicating that the increased size was likely due to increased hematopoietic cell populations rather than stromal components. The liver can also contribute to hematopoiesis. All OIM mice had reduced liver weight compared to WT, however in most cases this was proportional to their reduced bodyweight (Supplemental Figure 1). Male mice 7 weeks of age, the cohort that demonstrates the greatest degree of splenomegaly, show a small but significant increase in liver size in relation to bodyweight.

The observation of splenomegaly prompted us to evaluate hematopoietic lineages and their progenitors within bone marrow. Detailed flow cytometry analysis was performed on 7-week old mice. OIM mice generally had similar yields of bone marrow cells as WT controls, however sample collection was sometimes impaired by the presence of fractures or bone fragility. We therefore present all bone marrow data only as percentages of total bone marrow cells. The analysis indicated that there were no major changes in the frequency of early hematopoietic progenitor (LSK) cells (Figure 2A), the common lymphoid progenitor (Figure 2B), B cells (Figure 2C) or T cells (not shown). The common myeloid progenitor frequency was also unchanged (Figure 2D), however the distribution of more committed myeloid cells was altered specifically in male mice. Frequencies of both granulocyte-macrophage progenitors and megakaryocyte-erythroid progenitors were elevated in OIM males, as were CD11b<sup>+</sup> mature myeloid cells and Ly6G<sup>+</sup> granulocytes (Figure 2E–H). In contrast, Ter119<sup>+</sup> erythrocyte precursor frequency was decreased (Figure 2I). Further subdivision of the erythroblast populations indicated reductions in CD71<sup>+</sup> EryA and EryB precursors, but no change in the proportion of the most mature CD71<sup>-</sup> EryC cells (Supplemental Figure 2). Male OIM mice therefore have expansion of some components of the myeloid lineage within the bone marrow. Next we evaluated the frequency of immature OCPs (lymphoid<sup>-</sup> CD11b<sup>-/lo</sup> CD115<sup>+</sup> CD117<sup>+</sup>) using an established gating strategy (Figure 3A) [14]. There were no consistent differences in the frequency of OCPs within the bone marrow (Figure 3B). The altered osteoclast activity in OI can be at least partly attributed to abnormalities in osteoblast differentiation [12], but it is also possible that osteoclast differentiation in OI is increased independently of osteoblasts. Therefore we evaluated whether there were differences in osteoclast differentiation potential in purified osteoclast progenitors (CD11b<sup>-/lo</sup> CD115<sup>+</sup>) exposed to RANKL and M-CSF. The number of differentiated osteoclasts was increased in the OIM cultures at early time points, although the final number of osteoclasts produced was similar (Figure 3C). Osteoclasts did not develop from OIM OCPs in the absence of RANKL. Thus, we conclude that OIM mice do not show increased bone marrow OCP frequency, but bone marrow OCPs from OIM mice form osteoclasts more rapidly than cells derived from WT animals.

Next, we evaluated hematopoietic and OCP frequency in peripheral tissues. In the spleen, T cell frequency was unchanged in OIM mice, while B cell frequency was slightly but significantly reduced in males (Figure 4A–B). However, given the increased total spleen cell numbers in the OIM mice, this does not represent a change in the absolute number of B cells within OIM spleens (Supplemental table 2). We did not see changes in early hematopoietic progenitor cell (LSK) frequency in the spleen (data not shown). In contrast to the bone marrow, the spleen of male mice showed an increase in erythrocyte progenitor cell frequency (Figure 4C), but no change in Ly6G<sup>+</sup> granulocyte numbers (Supplemental table 2). The

CD11b<sup>hi</sup> myeloid cell frequency was significantly increased in OIM spleens in 7–9 week old male mice, however this change was lost by 17 weeks of age (Figure 4D). Female mice showed a transient increase in myeloid cell frequency in the spleen at 5 weeks of age, but no differences from WT following sexual maturity. The more defined peripheral OCP subset (lymphoid<sup>-</sup> CD11b<sup>hi</sup> CD115<sup>+</sup> Ly6C<sup>hi</sup>) showed very similar increases to the total CD11b<sup>hi</sup> population in male OIM animals (Figure 4E). We performed osteoclast differentiation assays using both total spleen cells and purified lymphoid<sup>-</sup> CD11b<sup>hi</sup> spleen cells from 7-week old animals. Larger numbers of osteoclasts were evident in OIM osteoclast cultures from whole spleen cells derived from male mice, however differences did not reach significance in females (Figure 5A). In both sexes we found increased osteoclast formation from purified OIM OCPs (Figure 5B). We also evaluated peripheral blood from these mice (Supplemental Figure 1). The frequencies of lymphoid cells and erythrocyte progenitors were unchanged, granulocyte frequency increased, and the CD11b<sup>hi</sup> myeloid population was enriched, however this change was only significant in 7-week-old males. There was no change in the frequency of CD115<sup>+</sup>Ly6C<sup>+</sup> OCPs (Supplemental Figure 1F). Collectively, our data indicate an increase in myeloid cells within peripheral tissues in young male OIM mice, with increased osteoclastogenic potential.

### 3.2 Inflammatory cytokine levels in OI

One mechanism that could explain the splenomegaly and expansion of the myeloid lineage is sustained inflammation, caused either by fractures, or, given that not all OIM mice have fractures evident by X-ray, other aspects of disordered bone and tissue turnover. Serum TNF $\alpha$  levels were elevated in OIM mice, significantly in females (Figure 6A). Serum IL1 $\alpha$  was also elevated, although again only in female mice (Figure 6B). IL6 was also measured, but was below the detection limit in the majority of samples (data not shown). These changes in cytokines indicate that systemic inflammation could be a factor contributing to the pathogenesis of OI.

### 3.3 Effect of anti-TNF $\alpha$ treatment in OIM

In order to target the inflammation occurring in OIM that is likely to contribute to high bone turnover, we treated OIM mice with murine TNFR2:Fc starting at 4–5 weeks of age and compared to vehicle-treated OIM and WT groups. Treatment was continued for 6 weeks. Weight gain throughout the study was consistent between all groups (Figure 7A), and OIM mice remained significantly smaller than their WT counterparts regardless of treatment group. OIM spleens were enlarged, as expected, in the vehicle-treated animals. Males did not show improvement in spleen size, however female spleens did show a reduction in size following treatment, although not a complete rescue in relation to WT mice (Figure 7B). Flow cytometry analysis of spleens failed to show consistently elevated frequencies of OCPs or myeloid cells in OIM, and the anti-TNF $\alpha$  treatment did not cause changes in cell frequency (data not shown). We hypothesized that reducing inflammation would reduce bone resorption. However, using serum CTX as a marker for bone resorption, we did not see a reduction following treatment, and CTX remained highly elevated compared to WT in both OI groups (Figure 7C). We evaluated bone parameters in these mice using DXA and  $\mu$ CT. Whole body BMD increased in all groups between the pre-treatment and endpoint scans (data not shown), however BMD remained significantly lower in all OIM groups, and was

not altered by the treatment (Figure 7D). Similar results were observed using femoral  $\mu$ CT, where OIM mice showed reductions in both trabecular and cortical bone volume that was not improved by TNFR2:Fc treatment (Figure 7E–F, Supplemental table 3). We also evaluated fracture frequency (Supplemental table 4). No fractures occurred in WT animals. The majority of OIM mice sustained at least one fracture prior to the start of treatment (87% of males, 70% of females). Some of these fractures healed during the treatment period, in both vehicle and TNFR2:Fc groups, particularly in the female mice. TNF $\alpha$ -neutralizing treatment failed to reduce fracture rates in OIM. Overall, while there is some evidence that TNFR2:Fc treatment may reduce inflammation in female OIM mice leading to reduced spleen size, our studies suggest that it does not improve the bone phenotype in these animals.

#### 4. Discussion

The primary site for hematopoietic development is the bone marrow, and the process is regulated by various cell types, including osteoblasts [30]. Therefore, although collagen defects are unlikely to affect hematopoiesis in a cell-autonomous manner, it is possible that changes in the osteoblast lineage, or matrix abnormalities, could affect hematopoietic differentiation. In the current study, we have found a number of alterations in the myeloid lineage in both bone marrow and spleen of OIM mice. These changes are mainly restricted to young adult male mice, with the exception of spleen size in relation to bodyweight, which was consistently increased in all ages examined and in both sexes. In line with the flow cytometry data, absolute spleen size was also increased only in young adult males. The splenomegaly was more severe soon after sexual maturity, particularly in males. We did not find evidence of extramedullary hematopoiesis, and the lack of changes in very early hematopoietic stem/progenitor populations suggest that the HSC niche is not dramatically altered by the collagen/bone abnormality. We did note changes in erythrocyte progenitor frequency that suggest extramedullary erythropoiesis in OIM. However, changes in erythroid populations within the spleen do not directly correlate with spleen size, and therefore are not sufficient to explain the splenomegaly in OIM (data not shown).

The splenomegaly and myeloid lineage expansion we observed may be indicative of low-level systemic inflammation. Similar changes are seen in mice with transgenic overexpression of TNF $\alpha$  [31]. Reduced bodyweight is also a feature of a number of inflammatory conditions [32, 33]. Inflammation may be related to the presence of fractures, but given that not all OIM animals have evident fractures and the spleen phenotype is very consistent, osteoblast abnormalities or disordered matrix may be important for promoting inflammation. Hematological abnormalities have not been reported in children with OI, and standard inflammatory markers such as C-reactive protein are usually within the normal range [7]. However given the variable severity in human OI, and genetic variation within humans, changes in inflammatory markers in peripheral circulation could fall within the normal clinical range. A recent study in children with OI found increased RANKL and DKK1 in serum, as well as increased OCP frequency [8]. Since myeloid cells may be both the source and targets of proinflammatory (or osteoclastogenic) factors, we expected increased frequency of the OCP subpopulation. We did not find significant differences in OCP frequency in peripheral blood of OIM mice, but frequency was increased in the spleen



of young males. Another study reported highly elevated prostaglandin E2 levels in untreated children with OI, a molecule produced in response to inflammation [7]. Interestingly, levels reduced following bisphosphonate treatment. We are not aware of any reports of splenomegaly in OI patients.

Our data suggest that the OIM microenvironment primes OCPs to differentiate more rapidly into osteoclasts. We found increased or more rapid osteoclastogenesis in isolated OIM bone marrow OCPs. Increased osteoblast-independent osteoclastogenesis has previously been reported in cells from both OIM and *Brl1* mice, although neither used such a highly purified progenitor population that could not have contained osteoblast lineage cells [4, 13]. Further studies are required to define the mechanism for this change. We also observed increased osteoclast formation in both total spleen and spleen OCPs. The increase in total spleen osteoclast formation appears to be a combination of both increased OCP frequency and activity. Peripheral OCPs are likely to be an important contributor to the osteoclast pool during states of inflammation or injury. It is unclear whether they are important to the pathogenesis of OI in the absence of fractures, but OIM mice certainly have dramatically increased bone resorption as evidenced by increased osteoclast numbers in vivo and extremely high CTX levels in their serum [2].

One factor that can contribute to inflammatory bone loss is TNF $\alpha$ . TNF $\alpha$  is a major mediator of disease in RA and other inflammatory conditions, and TNF $\alpha$  neutralizing therapies are widely used therapeutically. The effects of TNF $\alpha$  on bone and during healing are concentration-dependent, but at high doses it promotes osteoclast formation and bone resorption while inhibiting osteoblast differentiation, both of which could exacerbate the phenotype in OI [5, 34]. Previous studies indicated that TNF $\alpha$ , derived from the osteoblast lineage, contributed to increased osteoclastogenesis in vitro in OIM co-cultures [12]. TNF $\alpha$  expression was also found to be upregulated in peripheral blood cells in children with OI [8]. We found increased TNF $\alpha$  levels in OIM mice, although the increase reached statistically significant only in female mice. Clinical studies have shown that not all patients with active inflammatory arthritis have significantly elevated serum TNF $\alpha$  levels, but still respond to treatments targeting TNF $\alpha$ , suggesting that serum TNF $\alpha$  does not always reflect local increases in expression of this cytokine [35]. We therefore evaluated the effects of treatment with murine TNFR2:Fc, a TNF $\alpha$ -neutralizing therapy in OIM mice. Like TNFR2:Fc, the approved drug etanercept binds to TNF $\alpha$ . We therefore chose a dose approximately equivalent to the standard human etanercept dose used for RA treatment (0.5–1mg/kg) when converted using the body surface area normalization method [36]. A range of doses have been used in mouse treatment studies, and similar doses have been effective at reducing or preventing development of RA-like symptoms in mouse models of arthritis [31, 37]. Human etanercept is active in mice, but in this study we used the murine TNFR2:Fc which should avoid the potential for production of antibodies, which have been reported in some studies using high doses of etanercept in mice [37]. Unfortunately, the treatment regimen used in this study did not improve the bone phenotype in OIM mice. In females there was a reduction in the spleen size, suggesting that there was some anti-inflammatory effect of the treatment, but it was not sufficient to alter bone resorption. We treated a cohort of mice using the same protocol with a higher dose of TNFR2:Fc (25 $\mu$ g/g) that effectively reduced inflammation and improved the phenotype in a mouse model of cherubism [33]. However

this also failed to show any effect on CTX, bone parameters or spleen size in OIM (data not shown). Given that the phenotype in OIM appears to be more severe during growth, and the signs of inflammation reduce with age, it is unlikely that initiating treatment in older mice would prove beneficial. It is possible, however, that other treatments targeting inflammation, such as cyclooxygenase inhibitors, could improve inflammation and reduce bone turnover in OI.

We chose the OIM mouse for this study due to its well-established high bone turnover [2]. OIM has been widely used to characterize a variety of phenotypic features and evaluate various treatments. While it certainly mimics many features of human OI, it does not reflect an actual human mutation, and it is unusual in that it requires two copies of the *Col1a2* mutation in order to cause severe disease. It is likely that the hematopoietic and osteoclast lineage changes we have documented are specific to severe forms of OI, however further studies will be required to confirm this.

An interesting finding in this study was the sexual dimorphism in many aspects of the OIM phenotype. It is now well established that sex affects not only skeletal size and structure, particularly trabecular bone volume, but can also affect in vitro differentiation potential of both osteoblasts and osteoclasts [38, 39]. In addition to observing greater bone volume in males than females, we noted significant changes in myeloid cell frequency and peripheral OCPs in OIM males that were not seen in females. The hematopoietic phenotype was not evident in males until after sexual maturation (7 weeks old), however 5-week old OIM females showed increased myeloid cells in the spleen, but without the other changes seen in males. In contrast, surprisingly only females showed significantly elevated levels of TNF $\alpha$  and IL1 $\alpha$  in serum. We also observed a tendency toward higher fracture rate in OIM males, a trend that has been reported in previous studies as well as in a human cohort [40, 41]. The sexual dimorphism in the OIM phenotype is therefore more prevalent during early adulthood, but some differences are already evident by 5 weeks of age prior to sexual maturation. Some studies in OIM have pooled mice of both genders for evaluation of treatment approaches [42], and many have used animals of one gender only [24, 26, 43–45]. As noted in other recent studies, there are indications of sex-related differences in OI that may affect response to treatment that should be taken into account in future studies, particularly those targeting adolescents and adults [41, 46].

## 5. Conclusion

In conclusion, we have found age- and sex-related increases in myeloid cell frequency and peripheral OCP frequency, as well as persistent splenomegaly in the OIM model of osteogenesis imperfecta. In addition, OCPs from both bone marrow and spleen form osteoclasts more rapidly than WT counterparts. These changes suggest inflammation may be contributing to the elevated bone turnover and high bone resorption. However, targeting inflammation by TNF $\alpha$  neutralizing treatment failed to show a therapeutic effect in this model. Further studies are required to test the efficacy of other treatment options targeting inflammation and bone resorption, and OIM as a model of severe OI may be particularly useful in such investigation.

## Supplementary Material

Refer to Web version on PubMed Central for supplementary material.

## Acknowledgments

The authors thank Amgen for provision of murine TNFR2:Fc. We acknowledge Devin Shaheen for technical assistance. This work has been supported by NIH/NIAMS grant AR066218 to IK, and the Michael Geissman Fellowship from the Osteogenesis Imperfecta Foundation to BGM.

## References

1. Rauch F, Glorieux FH. Osteogenesis imperfecta. *Lancet*. 2004; 363:1377–85. [PubMed: 15110498]
2. Kalajzic I, Terzic J, Rumboldt Z, Mack K, Naprta A, Ledgard F, Gronowicz G, Clark SH, Rowe DW. Osteoblastic response to the defective matrix in the osteogenesis imperfecta murine (oim) mouse. *Endocrinology*. 2002; 143:1594–1601. [PubMed: 11956140]
3. Lisse TS, Thiele F, Fuchs H, Hans W, Przemeczek GKH, Abe K, Rathkolb B, Quintanilla-Martinez L, Hoelzlwimmer G, Helfrich M, Wolf E, Ralston SH, de Angelis MH. ER stress-mediated apoptosis in a new mouse model of osteogenesis imperfecta. *PLoS Genetics*. 2008; 4:e7. [PubMed: 18248096]
4. Uveges TE, Collin-Osdoby P, Cabral WA, Ledgard F, Goldberg L, Bergwitz C, Forlino A, Osdoby P, Gronowicz GA, Marini JC. Cellular mechanism of decreased bone in Brtl mouse model of OI: Imbalance of decreased osteoblast function and increased osteoclasts and their precursors. *Journal of Bone and Mineral Research*. 2008; 23:1983–1994. [PubMed: 18684089]
5. Lam J, Takeshita S, Barker JE, Kanagawa O, Ross FP, Teitelbaum SL. TNF- $\alpha$  induces osteoclastogenesis by direct stimulation of macrophages exposed to permissive levels of RANK ligand. *Journal of Clinical Investigation*. 2000; 106:1481–1488. [PubMed: 11120755]
6. Oakley I, Reece LP. Anesthetic implications for the patient with osteogenesis imperfecta. *AANA Journal*. 2010; 78:47–53. [PubMed: 20977129]
7. D'Eufemia P, Finocchiaro R, Celli M, Zambrano A, Tetti M, Villani C, Persiani P, Mari E, Zicari A. High levels of serum prostaglandin E2 in children with osteogenesis imperfecta are reduced by neridronate treatment. *Pediatr Res*. 2008; 63:203–206. [PubMed: 18091347]
8. Brunetti G, Papadia F, Tummolo A, Fischetto R, Nicastrò F, Piacente L, Ventura A, Mori G, Oranger A, Gigante I, Colucci S, Ciccarelli M, Grano M, Cavallo L, Delvecchio M, Faienza MF. Impaired bone remodeling in children with osteogenesis imperfecta treated and untreated with bisphosphonates: the role of DKK1, RANKL, and TNF- $\alpha$ . *Osteoporosis International*. 2016:1–11.
9. Camacho NP, Hou L, Toledano TR, Ilg WA, Brayton CF, Raggio CL, Root L, Boskey AL. The material basis for reduced mechanical properties in oim mice bones. *J Bone Miner Res*. 1999; 14:264–72. [PubMed: 9933481]
10. Chipman SD, Sweet HO, McBride DJ, Davisson MT, Marks SC, Shuldiner AR, Wenstrup RJ, Rowe DW, Shapiro JR. Defective pro alpha 2(I) collagen synthesis in a recessive mutation in mice: a model of human osteogenesis imperfecta. *Proceedings of the National Academy of Sciences of the United States of America*. 1993; 90:1701–1705. [PubMed: 8446583]
11. McBride DJ Jr, Shapiro JR, Dunn MG. Bone geometry and strength measurements in aging mice with the oim mutation. *Calcif Tissue Int*. 1998; 62:172–6. [PubMed: 9437052]
12. Li HT, Jiang X, Delaney J, Franceschetti T, Bilic-Curcic I, Kalinovsky J, Lorenzo JA, Grcevic D, Rowe DW, Kalajzic I. Immature osteoblast lineage cells increase osteoclastogenesis in osteogenesis imperfecta murine. *American Journal of Pathology*. 2010; 176:2405–2413. [PubMed: 20348238]
13. Zhang H, Doty SB, Hughes C, Dempster D, Camacho NP. Increased resorptive activity and accompanying morphological alterations in osteoclasts derived from the Oim/Oim mouse model of osteogenesis imperfecta. *Journal of Cellular Biochemistry*. 2007; 102:1011–1020. [PubMed: 17668424]

14. Jacquin C, Gran DE, Lee SK, Lorenzo JA, Aguila HL. Identification of multiple osteoclast precursor populations in murine bone marrow. *Journal of Bone and Mineral Research*. 2006; 21:67–77. [PubMed: 16355275]
15. Jacome-Galarza CE, Lee SK, Lorenzo JA, Aguila HL. Identification, characterization, and isolation of a common progenitor for osteoclasts, macrophages, and dendritic cells from murine bone marrow and periphery. *Journal of Bone and Mineral Research*. 2013; 28:1203–1213. [PubMed: 23165930]
16. Dwan K, Phillipi CA, Steiner RD, Basel D. Bisphosphonate therapy for osteogenesis imperfecta. *Cochrane Database Syst Rev*. 2016; 10:CD005088. [PubMed: 27760454]
17. Rijks EB, Bongers BC, Vlemmix MJ, Boot AM, van Dijk AT, Sakkers RJ, van Brussel M. Efficacy and safety of bisphosphonate therapy in children with osteogenesis imperfecta: A systematic review. *Horm Res Paediatr*. 2015; 84:26–42. [PubMed: 26021524]
18. Land C, Rauch F, Glorieux FH. Cyclical intravenous pamidronate treatment affects metaphyseal modeling in growing patients with osteogenesis imperfecta. *J Bone Miner Res*. 2006; 21:374–9. [PubMed: 16491284]
19. Munns CF, Rauch F, Zeitlin L, Fassier F, Glorieux FH. Delayed osteotomy but not fracture healing in pediatric osteogenesis imperfecta patients receiving pamidronate. *J Bone Miner Res*. 2004; 19:1779–86. [PubMed: 15476577]
20. Hoyer-Kuhn H, Franklin J, Allo G, Kron M, Netzer C, Eysel P, Hero B, Schoenau E, Semler O. Safety and efficacy of denosumab in children with osteogenesis imperfecta—a first prospective trial. *J Musculoskelet Neuronal Interact*. 2016; 16:24–32. [PubMed: 26944820]
21. Grafe I, Alexander S, Yang T, Lietman C, Homan EP, Munivez E, Chen Y, Jiang MM, Bertin T, Dawson B, Asuncion F, Ke HZ, Ominsky MS, Lee B. Sclerostin antibody treatment improves the bone phenotype of *Crtp*<sup>-/-</sup> mice, a model of recessive osteogenesis imperfecta. *Journal of Bone and Mineral Research*. 2016
22. Jacobsen CM, Barber LA, Ayturk UM, Roberts HJ, Deal LE, Schwartz MA, Weis M, Eyre D, Zurakowski D, Robling AG, Warman ML. Targeting the LRP5 pathway improves bone properties in a mouse model of osteogenesis imperfecta. *J Bone Miner Res*. 2014; 29:2297–306. [PubMed: 24677211]
23. Jacobsen CM, Schwartz MA, Roberts HJ, Lim KE, Spevak L, Boskey AL, Zurakowski D, Robling AG, Warman ML. Enhanced Wnt signaling improves bone mass and strength, but not brittleness, in the *Col1a1*<sup>+/mov13</sup> mouse model of type I Osteogenesis Imperfecta. *Bone*. 2016; 90:127–132. [PubMed: 27297606]
24. Sinder BP, Eddy MM, Ominsky MS, Caird MS, Marini JC, Kozloff KM. Sclerostin antibody improves skeletal parameters in a *Brtl*<sup>+</sup> mouse model of osteogenesis imperfecta. *Journal of Bone and Mineral Research*. 2013; 28:73–80. [PubMed: 22836659]
25. Sinder BP, Salemi JD, Ominsky MS, Caird MS, Marini JC, Kozloff KM. Rapidly growing *Brtl*<sup>+</sup> mouse model of osteogenesis imperfecta improves bone mass and strength with sclerostin antibody treatment. *Bone*. 2015; 71:115–123. [PubMed: 25445450]
26. Grafe I, Yang T, Alexander S, Homan EP, Lietman C, Jiang MM, Bertin T, Munivez E, Chen YQ, Dawson B, Ishikawa Y, Weis MA, Sampath TK, Ambrose C, Eyre D, Bachinger HP, Lee B. Excessive transforming growth factor-beta signaling is a common mechanism in osteogenesis imperfecta. *Nature Medicine*. 2014; 20:670–675.
27. Kawai VK, Stein CM, Perrien DS, Griffin MR. Effects of anti-tumor necrosis factor agents on bone. *Current Opinion in Rheumatology*. 2012; 24:576–585. [PubMed: 22810364]
28. Saban J, King D. PCR genotyping of oim mutant mice. *Biotechniques*. 1996; 21:190–192. [PubMed: 8862795]
29. Koulonis M, Pop R, Porpiglia E, Shearstone JR, Hidalgo D, Socolovsky M. Identification and analysis of mouse erythroid progenitors using the CD71/TER119 flow-cytometric assay. *J Vis Exp*. 2011
30. Visnjic D, Kalajzic Z, Rowe DW, Katavic V, Lorenzo J, Aguila HL. Hematopoiesis is severely altered in mice with an induced osteoblast deficiency. *Blood*. 2004; 103:3258–64. [PubMed: 14726388]

31. Li P, Schwarz EM, O'Keefe RJ, Ma L, Looney RJ, Ritchlin CT, Boyce BF, Xing L. Systemic tumor necrosis factor  $\alpha$  mediates an increase in peripheral CD11b<sup>high</sup> osteoclast precursors in tumor necrosis factor  $\alpha$ -transgenic mice. *Arthritis & Rheumatism*. 2004; 50:265–276. [PubMed: 14730625]
32. Keffer J, Probert L, Cazlaris H, Georgopoulos S, Kaslaris E, Kioussis D, Kollias G. Transgenic mice expressing human tumour necrosis factor: a predictive genetic model of arthritis. *EMBO J*. 1991; 10:4025–31. [PubMed: 1721867]
33. Yoshitaka T, Ishida S, Mukai T, Kittaka M, Reichenberger EJ, Ueki Y. Etanercept administration to neonatal SH3BP2 knock-in cherubism mice prevents TNF- $\alpha$ -induced inflammation and bone loss. *Journal of Bone and Mineral Research*. 2014; 29:1170–1182. [PubMed: 24978678]
34. Gilbert LC, Chen H, Lu X, Nanes MS. Chronic low dose tumor necrosis factor-alpha (TNF) suppresses early bone accrual in young mice by inhibiting osteoblasts without affecting osteoclasts. *Bone*. 2013; 56:174–183. [PubMed: 23756233]
35. Schulz M, Dotzlaw H, Neeck G. Ankylosing spondylitis and rheumatoid arthritis: serum levels of TNF-alpha and its soluble receptors during the course of therapy with etanercept and infliximab. *Biomed Res Int*. 2014; 2014:675108. [PubMed: 24783218]
36. Reagan-Shaw S, Nihal M, Ahmad N. Dose translation from animal to human studies revisited. *FASEB J*. 2008; 22:659–61. [PubMed: 17942826]
37. Yi H, Kim J, Jung H, Rim YA, Kim Y, Jung SM, Park SH, Ju JH. Induced production of anti-etanercept antibody in collagen-induced arthritis. *Mol Med Rep*. 2014; 9:2301–8. [PubMed: 24718553]
38. Zanotti S, Kalajzic I, Aguila HL, Canalis E. Sex and genetic factors determine osteoblastic differentiation potential of murine bone marrow stromal cells. *PLoS One*. 2014; 9:e86757. [PubMed: 24489784]
39. Ding Z, Wang Q, Pan X, Zhu Q, Lu H, Wang K, Ni X, Lu Y, Gu J. Expression of receptor activator of nuclear factor-kappaB ligand is related to sex differences in collagen-induced arthritis. *Int Immunopharmacol*. 2015; 28:892–6. [PubMed: 25863233]
40. Wekre LL, Eriksen EF, Falch JA. Bone mass, bone markers and prevalence of fractures in adults with osteogenesis imperfecta. *Arch Osteoporos*. 2011; 6:31–8. [PubMed: 22207876]
41. Boskey AL, Marino J, Spevak L, Pleshko N, Doty S, Carter EM, Raggio CL. Are changes in composition in response to treatment of a mouse model of osteogenesis imperfecta sexdependent? *Clinical Orthopaedics and Related Research*. 2015; 473:2587–2598. [PubMed: 25903941]
42. Bargman R, Posham R, Boskey AL, DiCarlo E, Raggio C, Pleshko N. Comparable outcomes in fracture reduction and bone properties with RANKL inhibition and alendronate treatment in a mouse model of osteogenesis imperfecta. *Osteoporosis International*. 2012; 23:1141–1150. [PubMed: 21901481]
43. Perosky JE, Khoury BM, Jenks TN, Ward FS, Cortright K, Meyer B, Barton DK, Sinder BP, Marini JC, Caird MS, Kozloff KM. Single dose of bisphosphonate preserves gains in bone mass following cessation of sclerostin antibody in *Brtl*/+ osteogenesis imperfecta model. *Bone*. 2016; 93:79–85. [PubMed: 27641475]
44. Vanleene M, Shefelbine SJ. Therapeutic impact of low amplitude high frequency whole body vibrations on the osteogenesis imperfecta mouse bone. *Bone*. 2013; 53:507–14. [PubMed: 23352925]
45. DiGirolamo DJ, Singhal V, Chang X, Lee SJ, Germain-Lee EL. Administration of soluble activin receptor 2B increases bone and muscle mass in a mouse model of osteogenesis imperfecta. *Bone Research*. 2015; 3
46. Yao X, Carleton SM, Kettle AD, Melander J, Phillips CL, Wang Y. Gender-dependence of bone structure and properties in adult osteogenesis imperfecta murine model. *Annals of Biomedical Engineering*. 2013; 41:1139–1149. [PubMed: 23536112]

### Highlights

- Osteogenesis imperfecta murine (OIM) animals exhibit splenomegaly
- Young adult male OIM animals show expansion of the myeloid lineage in bone marrow and spleen
- Purified osteoclast progenitors from bone marrow and spleen of OIM mice show more rapid osteoclastogenesis than wild-type
- Despite increased inflammatory cytokine expression in female OIM serum, TNF $\alpha$  neutralizing treatment did not reduce bone resorption or improve bone parameters

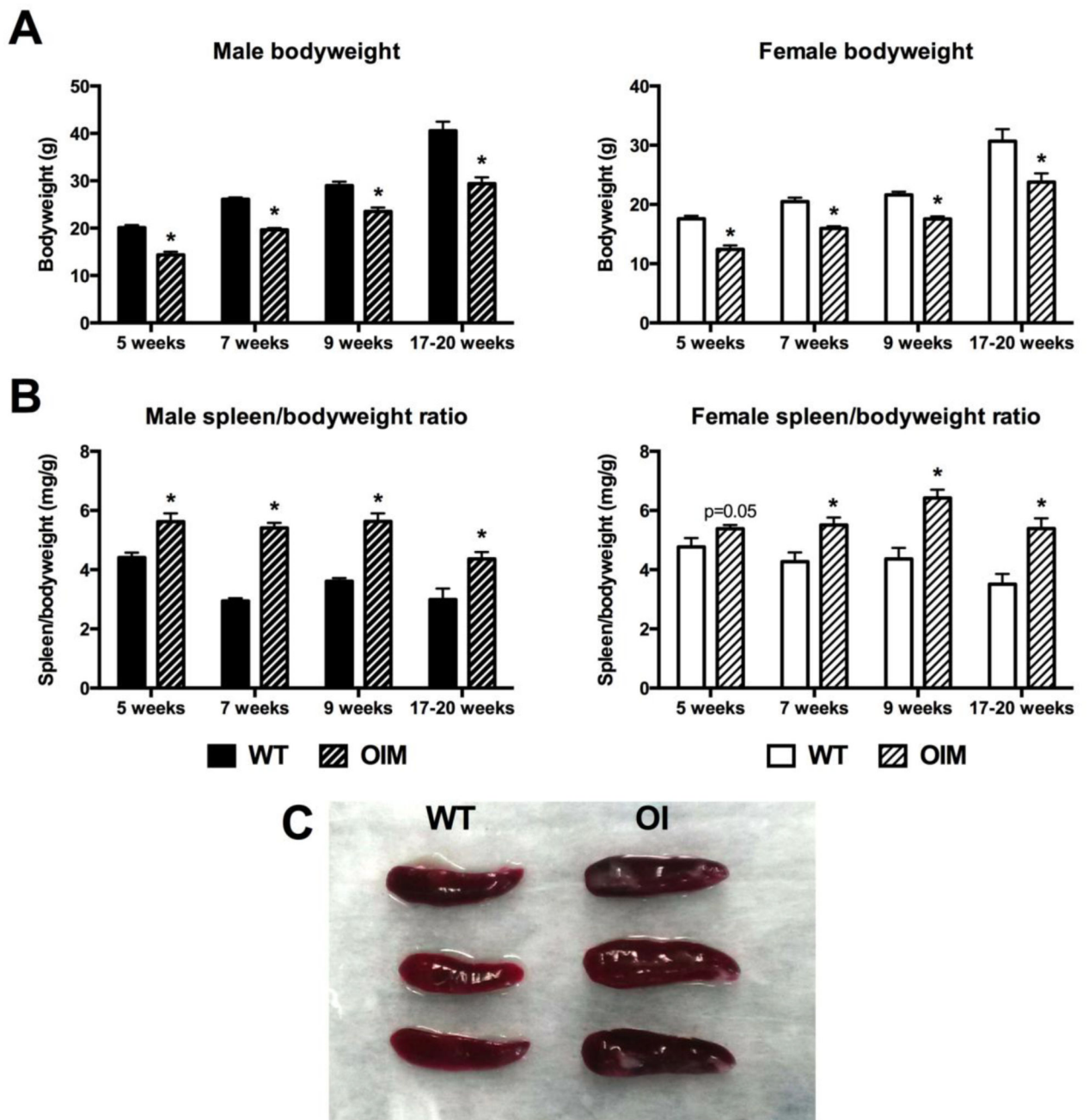


**Figure 1. Alterations in bodyweight and spleen size in OIM mice**

Bodyweight and spleen weight were measured in cohorts of OIM mice (OI) and their wild-type littermates (WT). (A) Bodyweight is shown in male and female mice of different ages. n=23–24 for 7-week males, and n=4–11 for other groups. (B) Spleen weight corrected for bodyweight is shown in the same groups of mice. (C) Spleens from 7 week old OIM males are enlarged compared to WT controls. \* p<0.05 compared to WT control.

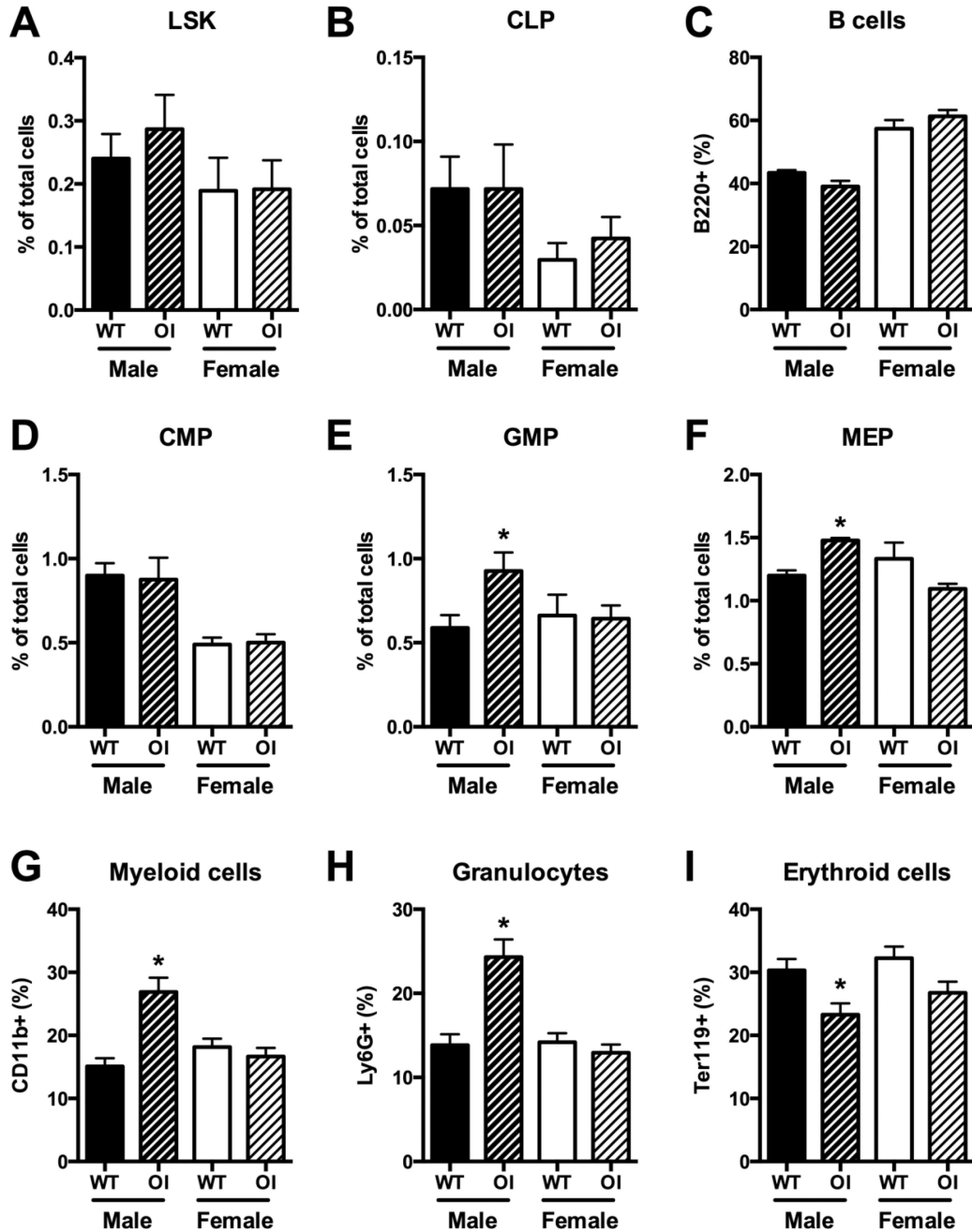


**Figure 2. OIM mice have increased frequency of myeloid lineage cells in bone marrow**  
 The frequency of different cell populations within the bone marrow of 7-week old WT and OI mice was evaluated by flow cytometry (n=5–6). Data are shown for (A) Lin<sup>-</sup> Sca1<sup>+</sup> cKit<sup>+</sup> (LSK) hematopoietic progenitor cells; (B) common lymphoid progenitors (CLP), Lin<sup>-</sup> Sca1<sup>+</sup> cKit<sup>int</sup> IL7R<sup>+</sup>; (C) B cells, B220<sup>+</sup>; (D) common myeloid progenitors (CMP), Lin<sup>-</sup> Sca1<sup>-</sup> cKit<sup>+</sup> CD34<sup>+</sup> CD16<sup>lo</sup>; (E) granulocyte macrophage progenitors (GMP), Lin<sup>-</sup> Sca1<sup>-</sup> cKit<sup>+</sup> CD34<sup>+</sup> CD16<sup>hi</sup>; (F) megakaryocyte erythroid progenitors (MEP), Lin<sup>-</sup> Sca1<sup>-</sup> cKit<sup>+</sup> CD34<sup>-</sup> CD16<sup>-</sup>; (G) myeloid cells, CD11b<sup>+</sup>; (H) granulocytes, Ly6G<sup>+</sup>; and (I) erythrocyte progenitors, Ter119<sup>+</sup>. \* p<0.05 compared to WT control.



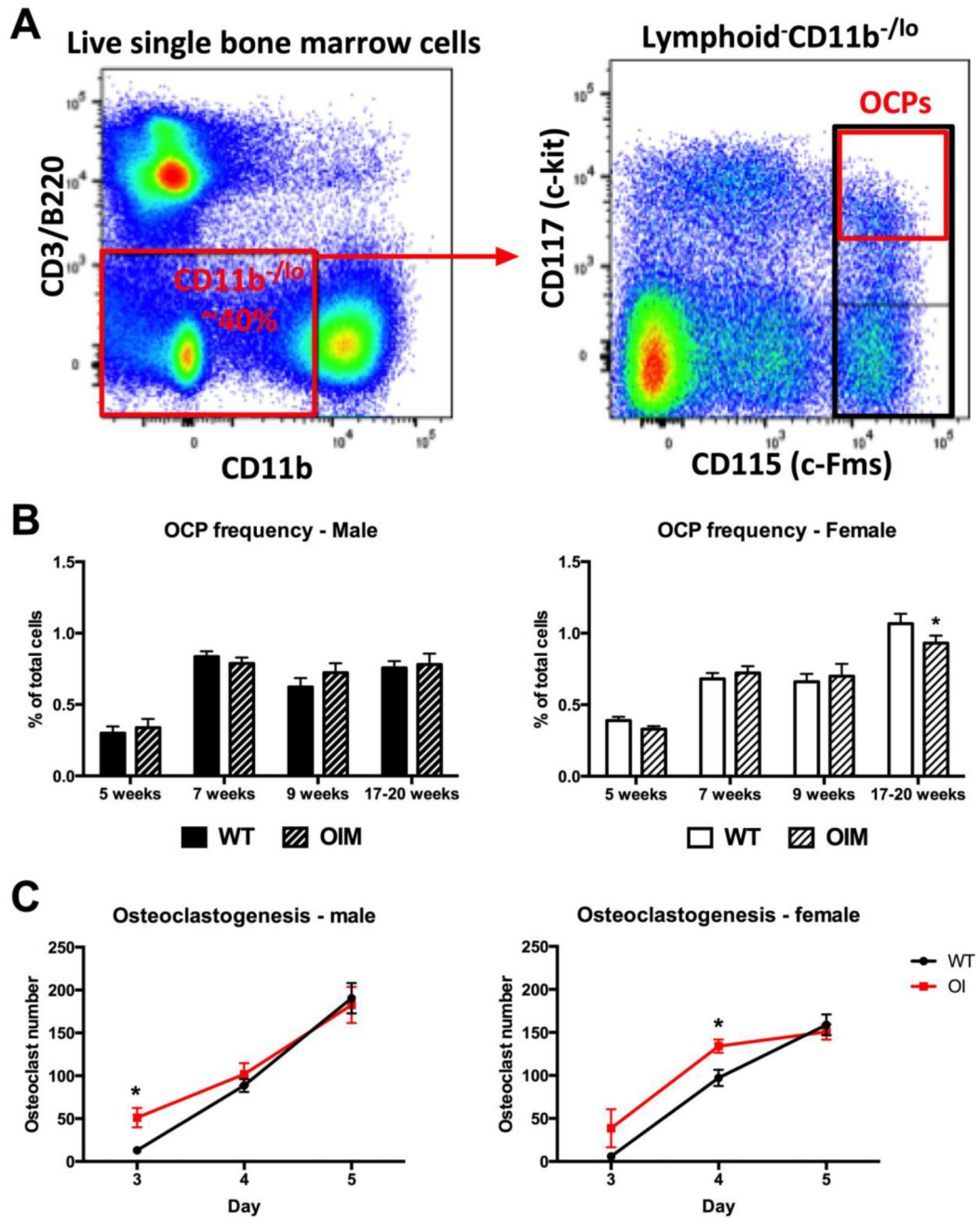


**Figure 3. Osteoclast precursor frequency and differentiation potential in bone marrow**  
 (A) Osteoclast progenitors (OCP) were identified using the indicated gating strategy. Purified OCPs are identified as shown in the red box in the right plot. For sorting of OCPs, the larger population identified by the black box was used. (B) Bone marrow OCP frequency in male and female mice of different ages, n=3–10. (C) Osteoclast number following culture of lymphoid<sup>-</sup> CD11b<sup>-/lo</sup> CD115<sup>+</sup> cells with RANKL and M-CSF. Data are pooled from 6 (male) or 4 (female) independent cultures each with 8 wells/group. \* p<0.05 compared to WT control.

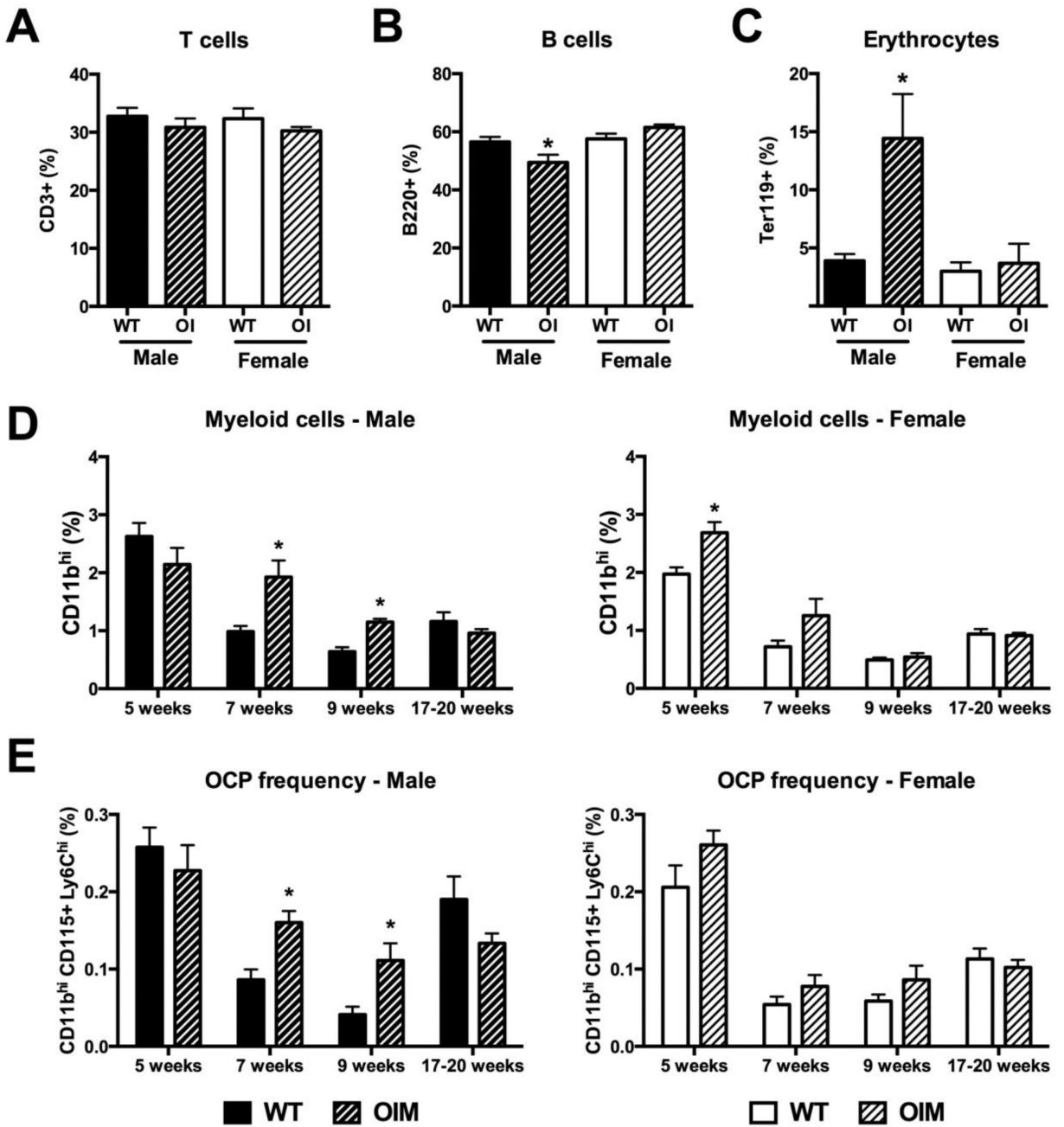


**Figure 4. OIM mice have increased osteoclast progenitors in the spleen**  
 Flow cytometry analysis was performed on spleen cells from WT and OI mice. Seven-week old animals (n=5–6) were used to evaluate changes in mature lineages including (A) T cells; (B) B cells; and (C) erythrocyte progenitors. Cohorts of male and female mice at different ages were used to evaluate the frequency of (D) myeloid lineage cells, CD11b<sup>hi</sup>; and (E) peripheral osteoclast progenitors (OCP), lymphoid<sup>-</sup> CD11b<sup>hi</sup> CD115<sup>+</sup> Ly6C<sup>+</sup>. n=4–10. \* p<0.05 compared to WT control.

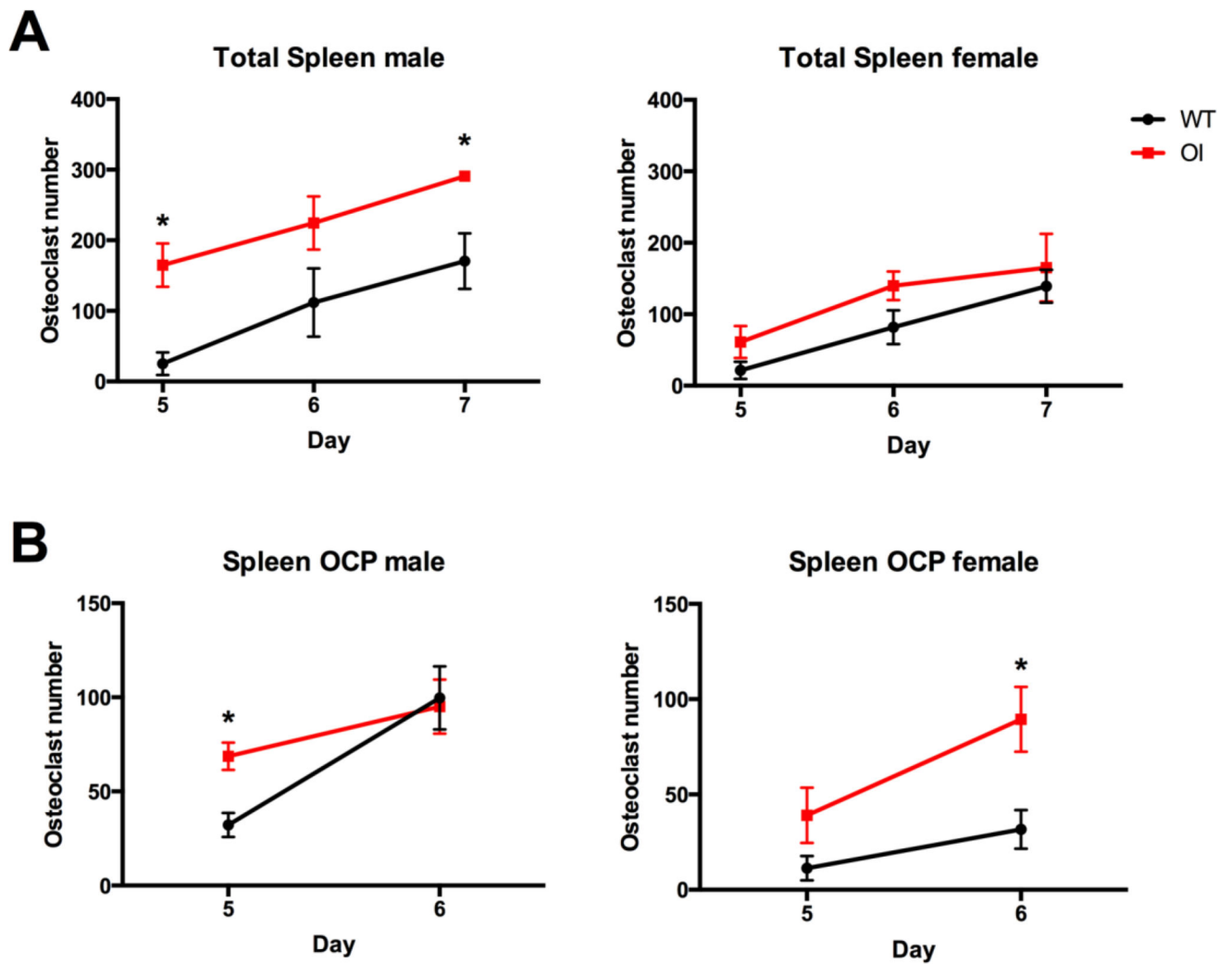


**Figure 5. Increased osteoclastogenesis from OIM spleen cells**  
 Osteoclast differentiation stimulated by M-CSF and RANKL was performed using (A) total spleen cells, and (B) sorted lymphoid<sup>-</sup> CD11b<sup>hi</sup> cells enriched for osteoclast progenitors and osteoclast number per well quantified. Data for each point are pooled from 4 independent cultures. \*  $p < 0.05$  compared to WT control.

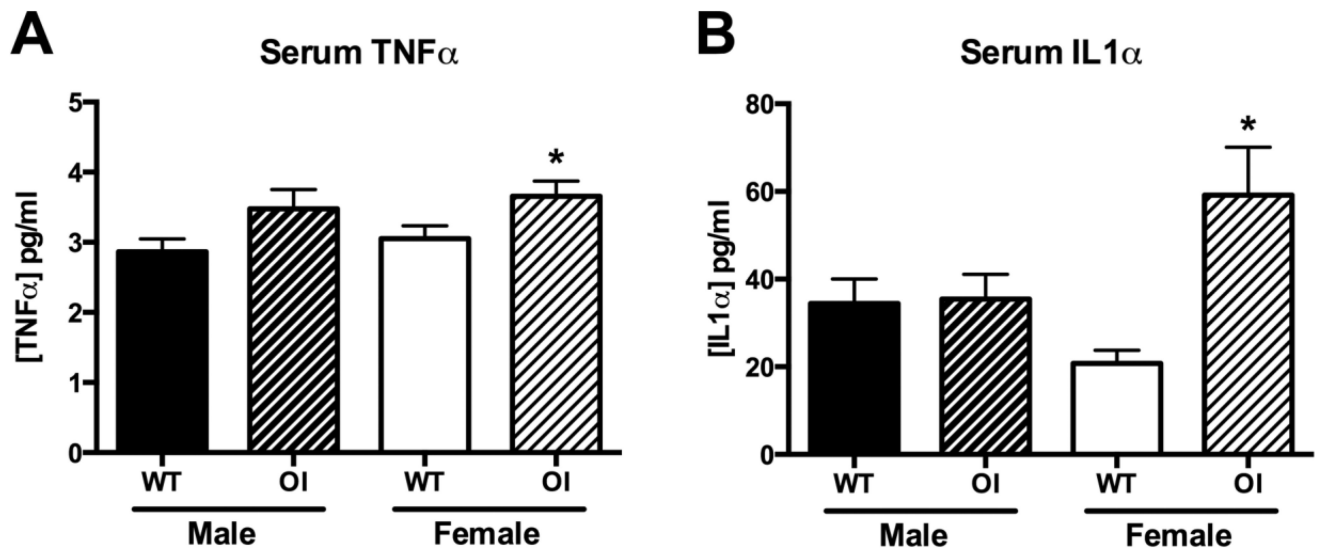


**Figure 6. Serum cytokine concentrations in OIM**

Serum levels of (A) TNF $\alpha$ , and (B) IL1 $\alpha$ , were measured by ELISA. Animals were 7–9 weeks of age at the time of serum collection, n=6–22. \* p<0.05 compared to WT control.

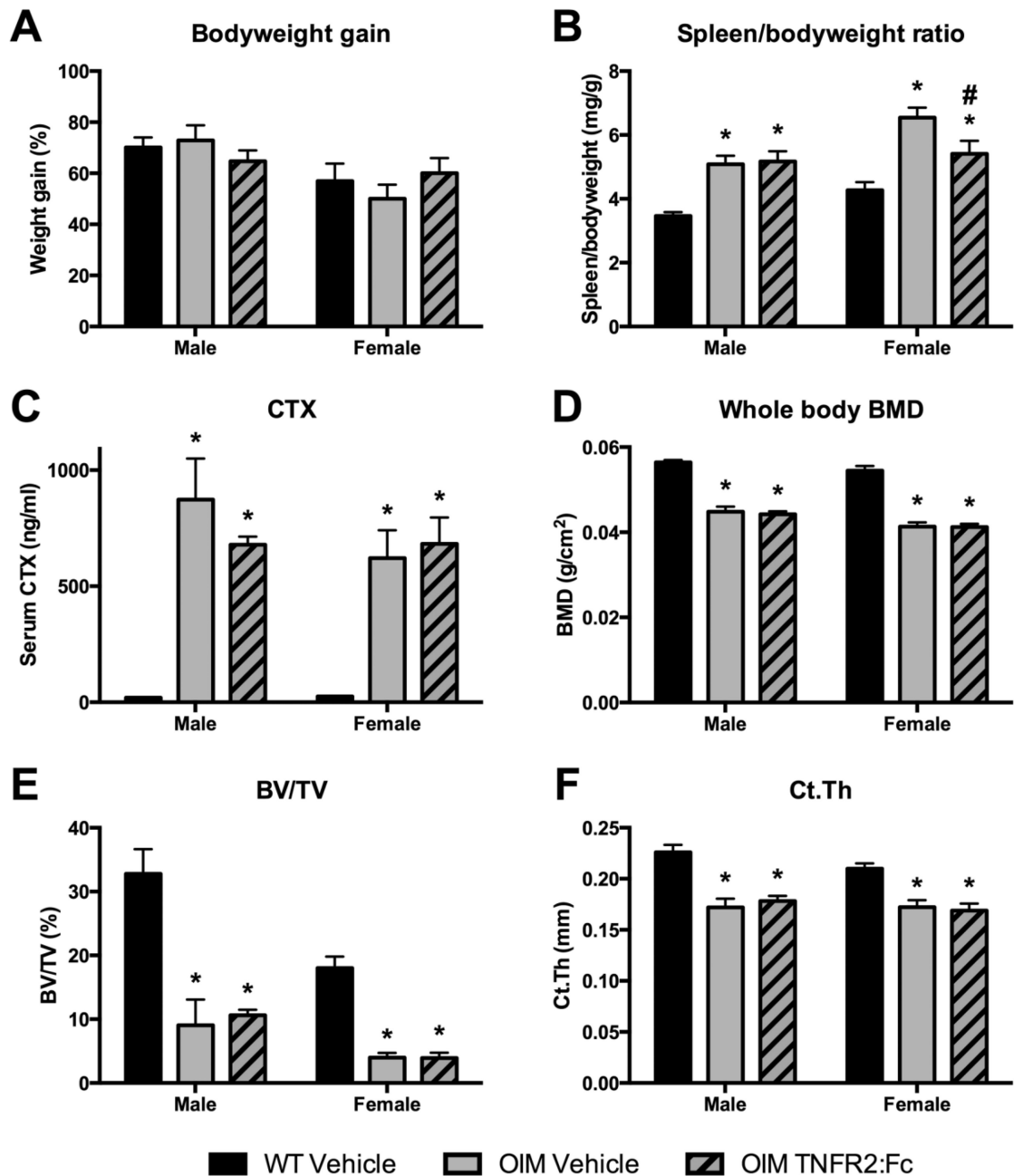


**Figure 7. Effect of TNF $\alpha$  neutralizing treatment on OIM phenotype**  
Mice were given vehicle or TNFR2:Fc twice weekly for 6 weeks. (A) Bodyweight increased in all groups, shown as % gain from initial weight. Other data were collected at sacrifice: (B) Spleen weight (corrected for bodyweight); (C) Serum CTX; (D) whole body bone mineral density (BMD); (E) femoral trabecular bone volume/total volume (BV/TV) and (F) cortical thickness (Ct.Th) as determined by  $\mu$ CT. n=8–14 for A–D and 4–9 for  $\mu$ CT data. \* p<0.05 compared to WT control; # p<0.05 compared to OIM vehicle.